INFLUENCE OF SI/AL RATIOS ON THE PROPERTIES OF COPPER BEARING ZEOLITES WITH DIFFERENT FRAMEWORK TYPES

Karolina MADUNA, Narendra KUMAR, Dmitry Yu. MURZIN

Abstract: Several copper containing zeolite based catalysts with different initial Si/Al and different zeolite support (types MCM-22, FAU, BETA) were synthesized or prepared from commercial precursors in a powdered and pelleted form via a direct hydrothermal synthesis and ion exchange method, and then subsequently characterized for the evaluation of their chemical, surface and catalytic properties. The characterization of the zeolites, which included the analysis of their morphological and acid-base properties, was performed by using various techniques such as the N2 physisorption, Pyridine-FTIR, XRD, SEM-EDAX and TEM. The activity and stability of the prepared catalysts were tested in the catalytic screening in a catalytic wet peroxide oxidation of the model polyphenolic wastewater. The obtained results provided an insight into the cause-and-effect relationship between the silica to alumina ratio and its direct effect on the acidity and basicity of the prepared zeolites, as well as the indirect one on their morphology, textural and surface properties of both the parent zeolite and active metal component. The use of active catalysts resulted in successfully operating the process under mild conditions with low energy consumption. It was found that the copper and iron containing catalysts showed promising activity, while the stability of the active metal component still is and remains a challenge to obtain.

Keywords: acidity; catalytic wet peroxide oxidation; morphology; phenolic wastewater; surface properties; transition metals; zeolites

1 INTRODUCTION

Zeolitic metal aluminosilicate solids are successfully used as catalysts in many industrial fine and bulk chemicals processes such as pharmaceuticals manufacture, petroleum refining and basic petrochemistry due to their microporous three-dimensional framework structures and high activity coupled with good stability [1, 2]. Apart from their proven applicability in manufacturing and processing, zeolites have also shown a potential for use in a variety of other fields. One such area, wastewater treatment, strongly gains in importance due to the contemporary environmental concerns and the growing need for a high quality freshwater supply. The potential application of metal modified zeolites as catalysts in wastewater treatment processes such as advanced oxidation (AOP) and catalytic wet oxidation (CWO) has been vastly studied in the past decades. Such studies are only intensifying with the discovery of new zeolitic structures [3-6].

Among them, large pore zeolites such as FAU, BETA or MCM-22 have peeked interest for the use in the processes that deal with large organic molecules that can be found in environmental catalysis and applications such as the CWPO of organic compounds. Although the reports on the catalytic properties of zeolite and zeolite based catalysts in the CWPO of the industrial olive oil mill effluents are scarce [7-9], there are numerous studies of the model OOMW wastewater or single compounds aqueous solutions. As it was reported by Liotta et al. [5], transition metal exchanged (mostly iron and copper) zeolites of the FAU or MFI morphology exhibit promising results. However, there are still some open issues in connection to their stability such as resistance to the leaching of the active metal during the reaction. The leaching of the active metal components from redox molecular sieves catalysts in the liquid phase oxidation catalysis is considered to be the consequence of the strong complexing and solvolytic properties of oxidants (e.g. H_2O_2) and/or products (e.g. H_2O, ROH, RCO_2H). This leads to the deactivation and secondary contamination of the effluent both undesirable from the economic and ecological point of view. To have a utility on an industrial scale, the heterogeneous catalyst should be very robust with no or negligible leaching of the active components, therefore turning the focus in the catalyst development for the use in the CWPO on not only active but also stable catalysts, is a necessity.

Additionally, apart from a few recent reports [10, 11], most of the studies in the field are concentrating on the examination of the catalytic properties of the powdered catalysts for which mass transfer limitations can be neglected. However, in order to move from a laboratory scale to the development of a commercial CWPO process, more detailed studies with the pelletized or beaded catalysts should be conducted. In this case, mass transfer and diffusion processes in the boundary layer surrounding the catalyst pellet and in the pores of the catalyst, with the latter being more probable, should be considered.

Therefore, in the current research study, several zeolite based catalysts with different initial Si/Al ratios containing copper as an active metal component and different zeolite support (types MCM-22, FAU, BETA) were synthesized or prepared from commercial precursors in a powdered and pelleted form via direct hydrothermal synthesis and ion exchange method, and then subsequently characterized for an evaluation of their chemical, surface and catalytic properties.

2 MATERIALS AND METHODS
2.1 Zeolite preparation

In the first two cases, a series of proton forms of Na-BETA and Na-MCM-22 zeolites with varying Si/Al ratios were prepared by means of the thermal treatment of the ammonium form of commercial zeolite (BETA, Si/Al of 25,

150 and 300) and direct hydrothermal synthesis (MCM-22, Si/Al of 30, 50 and 100) according to the previously described procedures [12, 13]. The copper bearing zeolite based catalysts were prepared by means of ion exchange from metal salt aqueous solutions in order to obtain a low loading/high dispersion of copper over the parent zeolite. In the third case, a commercial pelleted zeolite catalyst of the FAU type (13X, pellet size ~0.63 mm) with high aluminium content (Si/Al ratio of 2.6) was used as a support during the preparation of the copper bearing 13X catalyst by using the same method of incorporation of the active metal cation incorporation: ion exchange.

2.2 Characterization methods

The textural characterization of the catalysts was performed by nitrogen physisorption at 77 K by using the Sorptomatic 1900 Carlo Erba instrument. Prior to the measurements, the samples were outgassed at 423 K for 3 h at a reduced pressure below 0.1 mbar. The specific surface area and pore volume calculations were performed by using the Dubinin's equation for microporous and the B.E.T. equation for mesoporous samples. The pore size distributions were acquired by using the Horvath-Kawazoe method.

The strength of the Brønsted and Lewis acid sites of the catalysts was measured with infrared spectroscopy (ATI Mattson FTIR) by using the pellet technique working in the range of wavenumbers of 4000–400 cm^{-1} with pyridine as a probe molecule [14]. The temperature programed desorption of pyridine was conducted by evacuation at three different temperatures (523, 623 and 723 K) to obtain a distribution of acid site strength. The spectral bands at 1545 and 1540 cm-1 were used for the identification and quantification of the Brønsted (BAS) and Lewis (LAS) acid sites by using the corresponding bands intensities and molar extinction coefficients proposed in [15, 16].

The morphology of the prepared material was studied by using the scanning electron microscopy (SEM) and transmission electron microscopy (TEM). The SEM analysis was performed on a carbon coated samples by using a LEO Gemini 1530 instrument equipped with a Thermo Scientific UltraDry Silicon Drift Detector (SDD). The transmission electron microphotographs were taken by the JEM-1400 Plus transmission electron microscope (TEM) operated at a 120 kV acceleration voltage. The powdered samples were suspended in 100% ethanol under ultrasonic treatment for 10 min. For each sample, a drop of ethanol suspension was deposited on a Cu fiber carbon grid (200 Mesh) and evaporated, thereafter the images were recorded.

The copper content in the catalysts was determined by UV/VIS (UV1600PC, Shimadzu) at 270 nm from the copper acetate solutions used during an ion exchange and by the SEM-EDAX analysis during the SEM morphological studies of the powdered samples analysing the multiple section areas of the spread sample across the sample holder cell.

2.3 Catalytic screenings

The catalytic screening of the synthesized zeolites was evaluated in a model test reaction: catalytic oxidation of model polyphenol (tyrosol or phenol) with hydrogen peroxide in aqueous solutions. The catalytic experiments were carried out in a 200 cm^3 glass batch reactor equipped with a pH electrode and a temperature sensor at the atmospheric pressure at 363 K with the catalyst loading of 0.5 g/L and the initial concentrations of hydrogen peroxide and model phenolic coumpounds of up to 0.1 mol dm^{-3} and 1000 ppm, respectively, according to the reactor setup presented in Fig. 1.
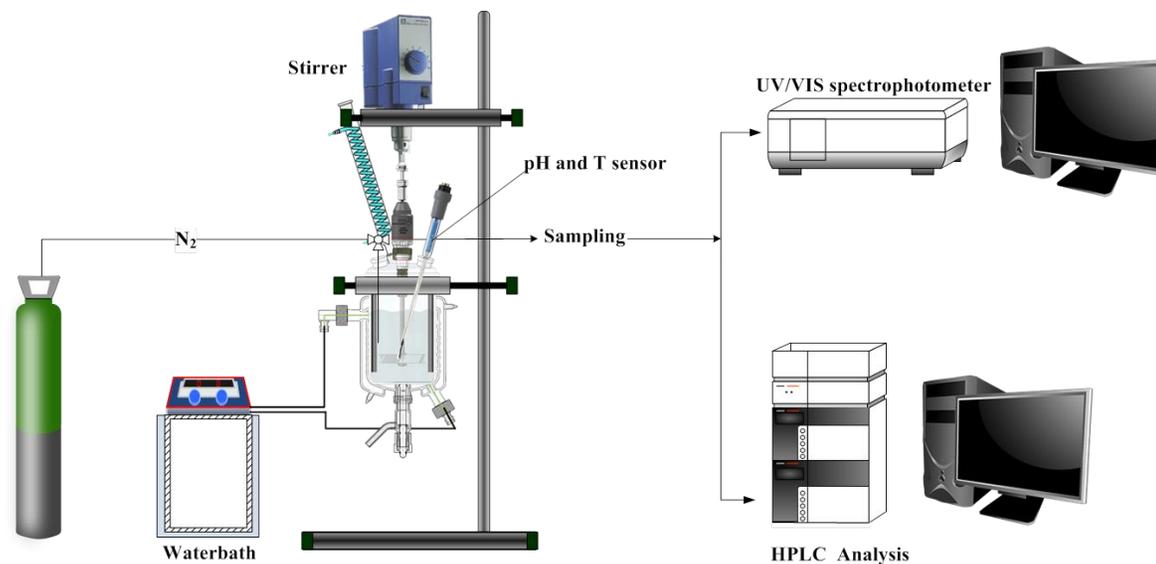
Figure 1 Process scheme of the reactor setup for catalytic screenings

To avoid the influence of the interphase mass transfer limitations on the observed kinetics, a high stirring speed (N=800 rpm) was employed and powder catalysts with particles sizes <125 μm were used during the runs. At regular time intervals, liquid samples were taken out of the reactor and analysed for monitoring the concentrations of tyrosol and hydrogen peroxide. For the quantification of the tyrosol content, Agilent Technologies Series 1100 HPLC was used equipped with an Ultra Techsphere ODS 5u analytical column (250×4.6 mm) connected to a diode array

(DAD) detector. A mixture of 0.5 wt. % of H_3PO_4 in water and methanol (70:30=v:v) was used as a mobile phase for the isocratic analysis at a flow rate of 0.8 ml min^{-1} and temperature of 308 K at λ=280 nm. The ammonium metavanadate UV-VIS spectrophotometric method at 450 nm adopted from Nogueira et al. [16] was used for the measurement of hydrogen peroxide concentrations. The copper content in the reaction mixture was measured by ICP-OES from the diluted reaction mixture solutions on a PerkinElmer, Optima 5300 DV instrument.
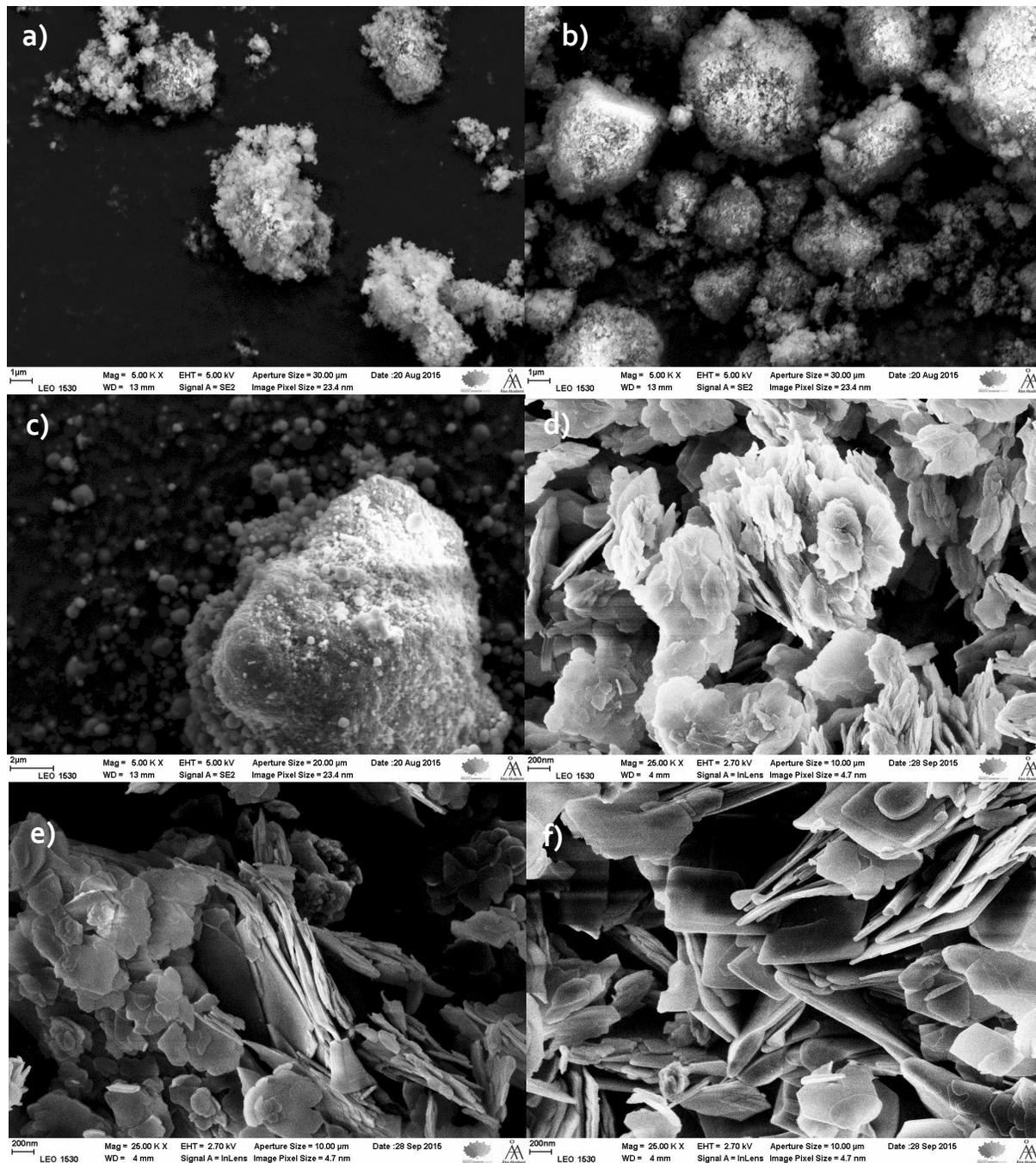
Figure 2 SEM images of Cu-BETA-25, Cu-BETA-150, Cu-BETA-300 (a-c) and Cu-MCM-22-30, Cu-CM-22-50, Cu-MCM-22-100 (d-f)

3 RESULTS AND DISCUSSION

The textural properties and respective active metal loadings of the prepared catalysts are presented in Tab. 1. All the catalysts exhibited similar textural properties, with high surface areas and large pore volumes. The active metal content of the catalysts was kept low except in the case of 13X zeolite which was several times higher due to the significantly higher acidity of the FAU zeolite type.

Table 1 Textural properties and respective active metal loadings of synthesized zeolites

Zeolite	Si/Al	Specific surface area $m^2\ g^{-1}$	Pore volume max $cm^3\ g^{-1}$	Copper content wt. %
Cu-H-BETA-25	25	705	0.59	1.1
Cu-H-BETA-150	150	649	0.68	1.3
Cu-H-BETA-300	300	783	0.40	0.9
Cu-H-MCM-22-30	30	612	0.41	1.03
Cu-H-MCM-22-50	50	522	0.30	0.90
Cu-H-MCM-22-100	100	270	0.17	0.25
Cu-13X pellet	2.6	618	0.34	8.0

The silica to alumina ratio significantly influenced textural properties, showing that both the pore volume and specific surface area decrease as the aluminium content in the parent zeolite gets lower due to the decrease in the presence of large opening cavities in the zeolites, and this can be observed both for BETA and MCM-22 zeolites. Similarly, the copper content decreased with the lower aluminium content in the zeolites indicating strongly that the active metal cation centres are directly dependant on the occurrence of aluminium 3+ sites in the zeolite framework.

The morphological studies of selected catalysts presented in Fig. 2 revealed typical crystallites structures for the BETA (round shaped), MCM-22 (layered leaflets) and FAU (needle shaped, not presented here) zeolite types. It can be observed that a slight decrease in the crystallite size occurs with the decrease of aluminium content in the zeolite of the specific framework type, which is specially pronounced for the MCM-22 zeolite whose particles decrease in average size from 0.9 µm for Si/Al=30 to 0.5 µm for Si/Al=100. Similarly, the copper particle size analysis by using the TEM images (not presented here) that was preformed on the Cu-MCM-22 zeolites showed that the active metal particles decrease in size with increasing Si/Al ratios. The Cu particle size distributions are decreasing in the range and size with the decrease in aluminium content having the average particle size of 6.3, 3.6 and 2.7 nm, respectively.

Table 2 Acidity of the prepared zeolite catalysts as the measured TPD pyridine desorption

Zeolite	Si/Al	Brønsted acidity, µmol/g			Lewis acidity, µmol/g		
		250 °C	350 °C	450 °C	250 °C	350 °C	450 °C
Cu-H-BETA-25	25	136	211	64	180	35	3
Cu-H-BETA-150	150	153	170	113	179	46	2
Cu-H-BETA-300	300	37	41	2	74	27	2
Cu-H-MCM-22-30	30	157	163	123	126	44	1
Cu-H-MCM-22-50	50	102	113	20	124	47	0
Cu-H-MCM-22-100	100	43	41	10	78	32	2

The Brønsted and Lewis acidities of the synthesized Cu-BETA and Cu-MCM-22 zeolites, as determined by the pyridine adsorption (FTIR), are presented in Tab. 2. As expected, the zeolite with the highest amount of aluminium showed to be the most acidic in terms of weak (523 K), medium (623 K) and strong (723 K) Brønsted acid sites. The total and the Brønsted acidity drop with the decrease in the aluminium content in the zeolites, while the Lewis acidity remains less pronounced and less affected by the change in the Si/Al ratios. The zeolites with the lowest aluminium content (Cu-H-BETA-300 and Cu-MCM-22-100) displayed the lowest total and Brønsted acidity, while the amount of the Lewis acid sites slightly increased when compared to the other samples.

The catalytic screening results are shortly summarized in Table 3. As it can be seen, the extent of the polyphenolic compound removal, as well as the decomposition of hydrogen peroxide over the catalyst surface during which the hydroxyl radicals are formed, strongly depend on the copper content of the catalyst, but also on the zeolite framework type, acidity and particle sizes of both the zeolites and active metal compound.

Table 3 Catalytic activity and copper leaching in the CWPO reactions with the Cu-MCM-22 and Cu-MCM-36 catalysts (T=60 °C, $c_{PPh,0}$= 500 mg/L, $c_{HP,0}$= 0.07 mol/L, m_{cat}=100 mg, N=800 rpm)

Zeolite	Si/Al	X_{PPh}, %	X_{HP}, %	γ_{Cu}, mg dm^{-3}
Cu-H-BETA-25	25	95	45	3
Cu-H-BETA-150	150	100	50	4
Cu-H-BETA-300	300	84	21	2
Cu-H-MCM-22-30	30	23	4	1
Cu-H-MCM-22-50	50	93	28	2
Cu-H-MCM-22-100	100	70	10	1
Cu-13X pellet	2.6	90	60	16

The stability of the catalysts showed to strongly depend on the yield of the reaction in terms of the conversion of polyphenol compounds. The more reaction progressed, the more of polyphenol was converted to low-molecular carboxylic acids that caused the decrease of the pH of the reaction mixtures, what is considered to be the main cause of the leaching of the active metal component of the catalyst, i.e. the copper particles. The leaching extent was also dependent on the acidity of the parent zeolite, showing that the catalysts that were more acidic in nature were also proved to be less stable.

4 CONCLUSIONS

The obtained results provided an insight into the cause-and-effect relationship between the silica to alumina ratio and its direct effect on the acidity and basicity of the prepared zeolites, as well as the indirect one on their morphology, textural and surface properties of both the parent zeolite and active metal component. As expected, the increase of the alumina content in the zeolite results in higher acidities of the material, which in turn affects the morphology and size of both the zeolite and active metal particles.

The use of active catalysts resulted in successfully operating the process under mild conditions with low energy consumption. It was found that copper and iron containing catalysts showed promising activity, while the stability of the active metal component still is and remains a challenge to obtain and further studies are required in order to understand the mechanisms of the deactivation process, as well as the development of the applicable stabilization techniques such as the postyinthesis chemical or thermal treatment. The catalyst pellet/particle size plays an important role in the activity in the CWPO showing that a decreasing of it occurs with the increase of the pellet size.

Acknowledgement(s)

Note: This research was presented at the International Conference MATRIB 2017 (29 June - 2 July 2017, Vela Luka, Croatia).

5 REFERENCES

[1] Čejka, J.; Centi, G.; Perez-Pariente, J.; Roth, W. Zeolite-based materials for novel catalytic applications: Opportunities, perspectives and open problems, J. Catal. Today 179 (2012) 2–15.

[2] Weitkamp, J. Zeolites and catalysis, Solid State Ionics 131 (2000) 175–188.

[3] Wang, N.; Zheng, T.; Zhang, G.; Wang, P. A review on Fenton-like processes for organic wastewater treatment, J. Environ. Chem. Eng. 4 (2015) 762–787.

[4] Navalon, S.; Alvaro, M.; Garcia, H. Heterogeneous Fenton catalysts based on clays, silicas and zeolites, Appl. Catal. B Environ. 99 (2010) 1–26.

[5] Liotta, L. F.; Gruttadauria, M.; Di Carlo, G.; Perrini, G.; Librando, V. Heterogeneous catalytic degradation of phenolic substrates: catalysts activity, J. Hazard. Mater. 162 (2009) 588–606.

[6] Busca, G.; Berardinelli, S.; Resini, C.; Arrighi, L. Technologies for the removal of phenol from fluid streams: a short review of recent developments, J. Hazard. Mater. 160 (2008) 265–288.

[7] Giordano, G.; Perathoner, S.; Centi, G.; De Rosa, S.; Granato, T.; Katovic, A.; Tagarelli, A.; Tripicchio, F. Wet hydrogen peroxide catalytic oxidation of olive oil mill wastewaters using Cu-zeolite and Cu-pillared clay catalysts, Catal. Today. 124 (2007) 240–246.

[8] Najjar, W.; Azabou, S.; Sayadi, S.; Ghorbel, A. Screening of Fe–BEA catalysts for wet hydrogen peroxide oxidation of crude olive mill wastewater under mild conditions, Appl. Catal. B Environ. 88 (2009) 299–304.

[9] Perathoner, S.; Centi, G. Wet hydrogen peroxide catalytic oxidation (WHPCO) of organic waste in agro-food and industrial streams, Top. Catal. 33 (2005) 207–224.

[10] Taran, O. P.; Zagoruiko, A. N.; Ayusheev, A. B.; Yashnik, S. A.; Prihod'ko, R. V.; Ismagilov, Z. R.; Goncharuk, V. V.; Valentin, N. Wet peroxide oxidation of phenol over Cu-ZSM-5 catalyst in a flow reactor. Kinetics and diffusion study, Chem. Eng. J. (2015), in press.

[11] Yan, Y.; Jiang, S.; Zhang, H. Efficient catalytic wet peroxide oxidation of phenol over Fe-ZSM-5 catalyst in a fixed bed reactor, Sep. Purif. Technol. 133 (2014) 365–374.

[12] Kumar, N.; Leino, E.; Mäki-Arvela, P.; Aho, A.; Käldström, M.; Tuominen, M.; Laukkanen, P.; Eränen, K.; Mikkola, J.-P.; Salmi, T.; Murzin, D. Y. Synthesis and characterization of solid base mesoporous and microporous catalysts: Influence of the support, structure and type of base metal, Microporous Mesoporous Mater. 152 (2012) 71–77.

[13] Käldström, M.; Kumar, N.; Heikkilä, T.; Yu. Murzin, D. Pillared H-MCM-36 mesoporous and H-MCM-22 microporous materials for conversion of levoglucosan: influence of varying acidity, Applied Catalysis A. General, 2011, 397, 13-21.

[14] Aho, A.; Kumar, N.; Eränen, K.; Salmi, T.; Hupa, M.; Yu. Murzin, D. Catalytic pyrolysis of biomass in a fluidized bed reactor: influence of acidity of H-beta zeolite, IChemE, part B, Process Safety and Environmental Protection, 2007, 85, 473-480.

[15] Emeis, C. A. Determination of Integrated Molar Extinction Coefficients for Infrared Absorption Bands of Pyridine Adsorbed on Solid Acid Catalysts, J. Catal. 141 (1993) 347–354.

[16] Nogueira, R.; Oliveira, M.; Paterlini, W. Simple and fast spectrophotometric determination of H(2)O(2) in photo-Fenton reactions using metavanadate, Talanta 66 (2005) 86–91.

Authors' contacts:

Karolina MADUNA
Faculty of Chemical Engineering and Technology,
Department of Reaction Engineering and Catalysis,
Marulićev trg 19, 10000 Zagreb, Croatia
kmaduna@fkit.hr

Åbo Akademi University, Department of Industrial Catalysis and Recation Engineering, Biskopsgatan 8, FI-20500 Turku, Finland

Narendra KUMAR
Dmitry Yu. MURZIN
Åbo Akademi University, Department of Industrial Catalysis and Recation Engineering, Biskopsgatan 8, FI-20500 Turku, Finland